

UAV-Assisted MEC Architecture for Collaborative Task Offloading in Urban IoT Environment

Subhrajit Barick, and Chetna Singhal, *Senior Member, IEEE*

Abstract—Mobile edge computing (MEC) is a promising technology to meet the increasing demands and computing limitations of complex Internet of Things (IoT) devices. However, implementing MEC in urban environments can be challenging due to factors like high device density, complex infrastructure, and limited network coverage. Network congestion and connectivity issues can adversely affect user satisfaction. Hence, in this article, we use unmanned aerial vehicle (UAV)-assisted collaborative MEC architecture to facilitate task offloading of IoT devices in urban environments. We utilize the combined capabilities of UAVs and ground edge servers (ESs) to maximize user satisfaction and thereby also maximize the service provider’s (SP) profit. We design IoT task-offloading as joint IoT-UAV-ES association and UAV-network topology optimization problem. Due to NP-hard nature, we break the problem into two subproblems: offload strategy optimization and UAV topology optimization. We develop a Three-sided Matching with Size and Cyclic preference (TMSC) based task offloading algorithm to find stable association between IoTs, UAVs, and ESs to achieve system objective. We also propose a K-means based iterative algorithm to decide the minimum number of UAVs and their positions to provide offloading services to maximum IoTs in the system. Finally, we demonstrate the efficacy of the proposed task offloading scheme over benchmark schemes through simulation-based evaluation. The proposed scheme outperforms by 19%, 12%, and 25% on average in terms of percentage of served IoTs, average user satisfaction, and SP profit, respectively, with 25% lesser UAVs, making it an effective solution to support IoT task requirements in urban environments using UAV-assisted MEC architecture.

Index Terms—Mobile edge computing, Internet of Things, unmanned aerial vehicles, task offloading, user satisfaction, service provider profit.

I. INTRODUCTION

The Internet of Things (IoT) technology supports numerous compelling applications with stringent requirements, such as real-time video analytics, augmented/virtual reality, video streaming, and automatic navigation [1]–[3]. These applications heavily rely on quick data processing for intelligent decision-making. However, IoT devices have limited processing resources and battery life that make it challenging to execute computation-intensive tasks. Mobile Edge Computing (MEC) is a potential paradigm that addresses the computing limitations of IoT devices [4]–[6]. By utilizing the computation and communication resources available at the network edge (e.g., cellular base stations, WiFi access points, and small-scale infrastructure), MEC enables IoT devices to execute computation-intensive applications by offloading them to the adjacent edge servers (ESs). This supports numerous advanced IoT applications by reducing service latency and improving service quality [7]–[10]. However, achieving dedicated wireless connections between IoTs and edge servers (ESs) may

not always be feasible in practical scenarios. This challenge becomes more prominent in urban environments [11]. The dense and varied cityscape, including tall buildings, creates physical barriers that hinder direct communication between IoT devices and edge resources. As a result, it becomes difficult to provide seamless connectivity and computing capabilities to all IoT devices. Deploying a large number of ESs across urban areas is a potential solution, but it requires careful planning, deployment, and management, which may increase the infrastructure implementation costs [12]. To overcome this, Unmanned aerial vehicles (UAVs) are used to dynamically enhance the quality of service (QoS) of MEC in IoT networks.

UAVs support mobility, on-demand deployment [13], [14], and the ability to establish line-of-sight links [15]–[17]. Collectively UAVs can provide efficient task distribution, adapt to the dynamic user demands, and enhance service quality [13], [18], [19]. These attributes enable UAVs to support IoT devices in performing computation-intensive and delay-critical tasks. They can be utilized as computing platforms to assist IoT device tasks [20], [21]. However, the UAVs have limited computational capacity, which may lead to significant delays while handling computational-intensive tasks [22]. Furthermore, as the task load increases, it brings adverse effects on both system performance and UAV’s battery lifetime [23]. UAV-enabled MEC systems, with UAVs acting as relays, can be used to improve user experience (based on service latency [9]) in IoT networks by offloading the computational tasks to more resourceful ground ESs [21], [24]. Unlike fixed relays, UAVs can quickly move to optimal locations, providing improved coverage and line-of-sight communication, especially in areas where buildings or infrastructure obstruct signal transmission. This mobility allows UAVs to effectively handle dynamic offloading demands in urban environments, where IoT device density and distribution vary over time—challenges that would be difficult for ground-based infrastructure to address alone.

However, in real-world networks, the edge resources are generally privately owned [25] and the service provider (SP) has to lease these resources to support diverse IoT applications [26]. Therefore, ensuring SP profit is equally important in UAV-assisted MEC networks along with user satisfaction [27]. Many recent studies in UAV-assisted MEC networks ([21]–[24]) emphasize the optimization of user satisfaction while neglecting the importance of SP profit. Thus, in this work, we model a MEC architecture that prioritizes both user satisfaction and SP profit. We consider a multi-UAV assisted task offloading architecture with UAVs acting as relays working in collaboration with ground ESs to improve the performance of MEC systems in urban IoT networks. Fig. 1 shows a sample scenario of the proposed multi-UAV assisted MEC system for IoT networks. To the best of our knowledge, UAV-assisted IoT task offloading in urban environments involving collaboration

S. Barick is with the Department of Information and Communication Technology, Manipal Institute of Technology, Manipal Academy of Higher Education, Manipal, India and C. Singhal is with INRIA, France.

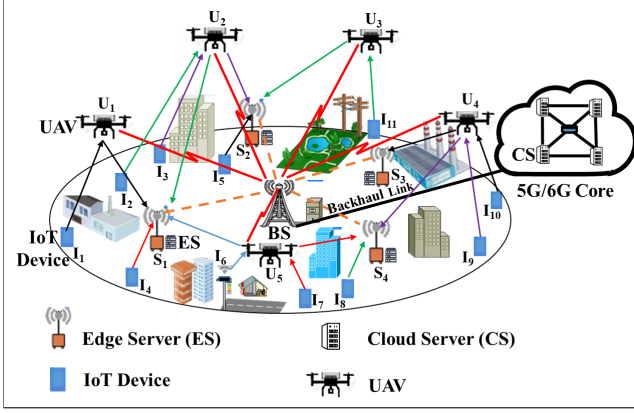


Fig. 1: Multi-UAV assisted MEC system for IoT network

References	Solution Approach	System-Cost, SP-Profit	Cyclic 3-sided Pref.	Adapt Real-Time	Multi-UAV Arch.	Urban network Scale	Latency	QoS
[7]	Reinforcement Learning	✓	✗	✓	✗	✗	✓	✓
[6]	Deep Reinforcement Learning	✓	✗	✗	✗	✗	✗	✓
[9]	Two-Sided Matching	✗	✗	✗	✗	✗	✓	✓
[8]	Three-Sided Matching	✓	✓	✓	✗	✗	✗	✓
[34]	Cyclic Stable Matching	✓	✓	✗	✗	✓	✓	✓
[10]	Multi-Stage Offloading	✗	✗	✗	✗	✓	✓	✓
[29], [32]	Multi-Agent Deep Reinforcement Learning	✓	✗	✓	✓	✓	✓	✓
[33]	Fixed Offloading	✓	✗	✗	✓	✓	✗	✓
[16], [27]	Random Offloading	✗	✗	✓	✓	✓	✓	✓
Our Approach	Three-Sided Matching w/ Cyclic Pref.	✓	✓	✓	✓	✓	✓	✓

TABLE I: Features Comparison between Proposed Strategy and state-of-the-art schemes between IoTs, UAVs, and ES owners, targeting to maximize the SP profit while meeting specific task requirements of IoTs has not been studied yet. Therefore, in this article, we propose an efficient task-offloading scheme to address this.

The key features of this article are summarized as follows:

- 1) A UAV-assisted MEC architecture to facilitate edge computing to IoT devices with limited connectivity.
- 2) IoT task offloading problem modeled as a joint IoT-UAV-ES association and topology optimization problem.
- 3) Optimization problem formulation to maximize SP profit while fulfilling task and service requirements.
- 4) Three-sided Matching with Size and Cyclic preference (TMSC) and K-means based heuristic algorithm to find efficient UAV topology and stable IoT-UAV-ES association.
- 5) Simulation-based performance evaluation with uniform and dataset based IoT distribution for varying numbers of IoTs and ESs, compares the proposed offloading with respect to state-of-the-art benchmark schemes in terms of percentage of served IoTs, number of UAVs deployed, average user satisfaction, and overall SP profit.

The remaining article is structured as follows: Section II reviews of related works. Section III presents the system model and analyzes the SP profit using a revenue-cost model. We model the task offloading process as a joint optimization of UAV topology and IoT-UAV-ES association problem. Section IV discusses our algorithmic approach to solving the profit maximization problem. Section V presents the performance evaluation and effectiveness of the proposed offloading scheme while section VI concludes the article.

II. RELATED WORKS

Task offloading helps to meet the computational requirements of resource-constrained heterogeneous IoT applications

[5]. This involves parameters like offloading latency, energy consumption, and system cost [6], [28]. Existing solutions that minimize the task execution delay in a MEC system are based on deep reinforcement learning [5] and optimization of service caching for multi-cell scenarios [28]. Collaboration between the edge nodes and BS reduces the end-to-end delay in cellular networks [10]. A collaboration between edge node and cloud server can further improve the efficiency of task offloading in heterogeneous cellular network [6]. An incentive framework for optimizing the system cost of mobile data offloading in such a system has the ES operator different from the network SP, and the SP pays for the offloading traffic to the ES [26].

However, these existing task-offloading strategies rely on consistent network connectivity between IoT devices and edge servers. In urban environments with high device density and complex infrastructure, network connectivity can be challenging [11]. This can lead to delays in data transmission, task execution, and overall performance degradation [29]. To overcome this, integration of UAVs into MEC networks in urban environments can provide communication support and assistance in task offloading services [21], [30]. The optimization of UAV deployment, user association, and resource allocation can improve the average offloading latency of the system [31], [32]. Additionally, the UAV trajectory and task allocations can be optimized to improve QoS of a MEC system [33]. Collaboration between UAV and edge cloud (EC) in the UAV-enabled MEC systems can enhance the system computation rate [34] and minimize service delay for IoT devices facing signal outage and shadowing [22].

A single UAV-assisted MEC solution only provides connectivity over a small area due to its limited coverage, battery life, and payload capacity. Therefore a multi-UAV enabled MEC system is a more efficient and reliable alternative for task offloading in urban environments [35]. A multi-UAV architecture can support on-demand task execution of computation-intensive applications on IoT devices [36]. Additionally, it can meet the low latency and QoS requirement of IoT applications [1], [7]. Collaboration between UAVs and BS helps in the efficient utilization of the available resources and improves the user experience in the MEC system [37]. Similarly, a collaboration between UAV and ESs can provide MEC services with reduced service latency to the IoT devices that are beyond the communication range of ECs by means of two-sided matching between the UAVs and ESs [38] or a cooperative deep reinforcement learning approach [39].

We note that the aforementioned studies have primarily focused on enhancing system performance from only the user's perspective, neglecting the SP perspective. However, the SP being profit-driven, needs to maximize the revenue while ensuring acceptable QoS for users [40]. We remark that the SP's perspective is equally important. Therefore, in this work, we propose a multi-UAV-assisted IoT edge-computing model considering both the user as well as the SP perspective. We have summarised the comparison of the proposed task offloading strategy with the other state-of-the-art schemes in terms of distinct features in Table I.

III. SYSTEM MODEL AND PROBLEM FORMULATION

Fig. 1 shows the system model for the proposed multi-UAV assisted IoT edge computing architecture with an underlying cellular 5G network. The system comprises of one macro base station (MBS), K UAVs, and L ESs. These components collaboratively facilitate task offloading service to M active IoT devices that may face difficulty in accessing ground ESs due to limited connectivity. Let $\mathcal{I} = \{I_1, I_2, \dots, I_M\}$, $\mathcal{U} = \{U_1, U_2, \dots, U_K\}$, and $\mathcal{S} = \{S_1, S_2, \dots, S_L\}$ denote the set of IoT devices, UAVs, and ESs in the system, respectively. Each active IoT device I_m has a computation-intensive task represented by the tuple $T_m = (D_m, C_m, \tau_m)$, where D_m (in bits) indicates the data size, C_m (in CPU cycles/bit) is the computing resource requirement to process single-bit data, and τ_m (in seconds) denotes the maximum tolerable task completion delay. We denote the system-level IoT task requirements as $\mathcal{T} = \{T_m, \forall m = 1, 2, \dots, M\}$. We consider that the tasks are offloaded to the ESs and not processed locally due to limited computing resources available at the IoT device. The UAVs are deployed as relays, which receive the task offloading requests from the IoTs and forward them to the appropriate ESs to meet IoTs' requirements. The ESs are deployed with the small cell 5G NR gNodeB that are privately owned (can support 5G private networks). The network SP leases and pays (to the ES owner) for the computing resources of these ESs to perform task-offloading of the IoT devices [26], [27]. Our primary objective is to maximize SP profit while ensuring seamless task offloading to a maximum number of IoTs, considering unique requirement of each IoT device.

We consider task offloading for a quasi-static scenario, where the operational duration is divided into numerous small intervals. Within each interval, we assume that the positions of IoTs and UAVs remain constant. We use a 3-D Cartesian coordinate system to represent the positions of IoTs, UAVs, and ESs within a small interval. The positions of IoT device I_m and ES S_l are denoted by $Q_{I_m} = (x_{I_m}, y_{I_m}, 0)$, and $Q_{S_l} = (x_{S_l}, y_{S_l}, 0)$, respectively, while the position of UAV U_k is denoted as $Q_{U_k} = (x_{U_k}, y_{U_k}, H)$, where H indicates the flying height of UAVs. Let $Q_I = \{Q_{I_m}, \forall m = 1, 2, \dots, M\}$, $Q_U = \{Q_{U_k}, \forall k = 1, 2, \dots, K\}$, and $Q_S = \{Q_{S_l}, \forall l = 1, 2, \dots, L\}$ be the set of positions of IoTs, UAVs, and ESs, respectively. The UAV altitude H is predefined based on the communication coverage area on the ground while limiting the experienced path loss [13], [17]. The positions of UAVs (x_{U_k}, y_{U_k}) are determined using the proposed algorithm (discussed in section V). With this, the communication and task offloading models are explained as follows.

A. Communication Model:

The communication between UAVs and ESs is facilitated by the MBS using Z physical resource blocks (PRBs). These PRBs are equally shared among all UAVs. Additionally, each UAV uses N_U PRBs (non-overlapping with MBS PRBs) to facilitate communication with the IoTs. We assume that each IoT device can be assigned a maximum of one PRB. Therefore, the maximum IoT user capacity of each UAV is considered as N_U .

Symbol	Physical significance
M, K, L, Z	Number of IoT devices, UAVs, ESs, and PRBs, resp.
$\mathcal{I}, \mathcal{U}, \mathcal{S}$	Set of IoT devices, UAVS, and ESs, resp.
T_m	Task generated at IoT device I_m
D_m, C_m	Data size, CPU cycle requirement of task T_m
τ_m	Maximum tolerable delay of task T_m
$\delta_{m,K,l}$	Offloading strategy of IoT device I_m
Δ	Set of Offloading strategies of all IoT devices
X_U, Y_U	Set of X- and Y- positions of UAVs
q_l	Processing capacity of ES S_l
\mathcal{F}	Set of processing capacities of ESs
\mathcal{T}	Set of task requirements of all IoTs
N_U	IoT user capacity of UAV
N_S	Task processing capacity of ES
$\Gamma_{m,k}; \tilde{\Gamma}_{k,l}$	SINR of I_m at U_k ; SINR of U_k at S_l
P_m	Transmitting power of IoT device I_m
P_k	Transmitting power of UAV U_k
$g_{m,k}, g_{k,l}$	Channel gain between I_m and U_k , U_k and S_l
N_0	Noise power
$r_{m,k}$	Data transmission rate between I_m and U_k
$r_{k,l}$	Data transmission rate between U_k and S_l
B_1, B_2	Bandwidth assigned to IoTs and UAVs, respectively
$t_{m,k,l}$	Offloading delay associated with the strategy $\delta_{m,k,l}$
$\gamma_{m,k,l}$	User satisfaction associated with the strategy $\delta_{m,k,l}$
$\mathcal{R}_{m,k,l}$	Revenue earned for offloading strategy $\delta_{m,k,l}$
$\mathcal{C}_{m,k,l}$	Cost incurred by SP for offloading strategy $\delta_{m,k,l}$
$\mathcal{P}_{m,k,l}$	Profit earned for the offloading strategy $\delta_{m,k,l}$
$CP(\delta_{m,k,l})$	Cost-performance of offloading strategy $\delta_{m,k,l}$

TABLE II: Notations and significance of symbols

We use the probabilistic LoS model to represent data transmission between the ground components (IoT or ESs) and UAVs [41]. We express the path loss between the ground component i and UAV j as

$$PL_{i,j} = \beta_0 d_{i,j}^2 [P_{i,j}^{LoS} \mu_{LoS} + P_{i,j}^{NLoS} \mu_{NLoS}] \quad (1)$$

where $\beta_0 = \left(\frac{4\pi f}{c}\right)^2$, f is the carrier frequency, c is the speed of light, $d_{i,j} = \sqrt{(x_i - x_j)^2 + (y_i - y_j)^2 + H^2}$ is the distance between the component i and UAV j , μ_{LoS} and μ_{NLoS} are the additional pathloss components for LoS and NLoS links, respectively. $P_{i,j}^{LoS}$ and $P_{i,j}^{NLoS}$ are the probabilities corresponding to the LoS and NLoS links, respectively, and are given as

$$P_{i,j}^{LoS} = \frac{1}{1 + a \exp(-b(\theta_{i,j} - a))} \quad (2)$$

$$P_{i,j}^{NLoS} = 1 - P_{i,j}^{LoS} \quad (3)$$

where a and b are the environment constants, and $\theta_{i,j} = \sin^{-1}\left(\frac{H}{d_{i,j}}\right)$ is the elevation angle of UAV j with respect to component i . The data rate between the two communicating components i and j is governed by the link Signal to Interference Noise Ratio (SINR), which is given as:

$$\Gamma_{i,j} = \frac{(P_i/PL_{i,j})}{\sum_{i'=1, i' \neq i}^{\eta} (P_{i'}/PL_{i',j}) + N_0}, 98 \quad (4)$$

where P_i is the transmitting power of i , N_0 is the noise power, and $\sum_{i'=1, i' \neq i}^{\eta} (P_{i'}/PL_{i',j})$ indicates the total interference power experienced at j due to channel reuse. Since we focus on dense urban scenario, the PRBs may be reused across

different clusters, and we carefully assign the PRBs to significantly reduce or even eliminate this co-channel interference under the given conditions. The task offloading rate is:

$$r_{i,j} = B_{i,j} \log(1 + \Gamma_{i,j}), \quad (5)$$

where $B_{i,j}$ is the communication bandwidth between ground component i and UAV j .

The SINR of IoT I_m while offloading task to UAV U_k is $\Gamma_{m,k}$ with $\eta = M$ and the transmitting distance of U_k from I_m as $d_{m,k} = \sqrt{[(x_{U_k} - x_{I_m})^2 + (y_{U_k} - y_{I_m})^2 + H^2]}$. Here, $B_{i,j} = B_1$, corresponds to the bandwidth of PRB assigned to I_m for offloading its task to U_k . Similarly, the SINR for UAV U_k while relaying an offloaded task to ES S_l is $\Gamma_{k,l}$ with $\eta = K$ and $d_{k,l} = \sqrt{[(x_{U_k} - x_{S_l})^2 + (y_{U_k} - y_{S_l})^2 + H^2]}$, the transmitting distance of U_k from S_l . Here, the UAV is assigned a bandwidth $B_{i,j} = B_2$ for relaying offloaded tasks to the ESs. The SINR corresponding to the IoT-UAV pair is measured at the UAV, while the SINR for the UAV-ES pair is measured at the ES [24]. These SINR values are then shared with the MBS over separate control channels. We denote the set of SINR values for all possible IoT-UAV and UAV-ES pairs as $\Gamma = \{\Gamma_{m,k}, \forall m, k\}$ and $\bar{\Gamma} = \{\Gamma_{k,l}, \forall k, l\}$ respectively.

B. Task Offloading Model:

The IoT device initiates the task offloading process by transferring its computation-intensive and delay-sensitive task to the associated UAV. The UAV then forwards the task to a suitable ES for further processing. The ESs are heterogeneous entities that exhibit heterogeneity in terms of their computing capacities. We represent the computing capacities of the ESs as a set $\mathcal{F} = \{q_1, q_2, \dots, q_l, \dots, q_L\}$, where q_l indicates the computing capacity (in CPU cycles/sec) of ES S_l . We assume that the computing resource of each ES is proportionally reserved for all the connected UAVs. The maximum number of tasks that each ES can handle is denoted as N_S and can be determined by taking the ratio of the average ES CPU cycles to the average CPU cycle requirements of IoT tasks in the system. If the ES CPU cycle capacity in the system is within the range $[q_{min}, q_{max}]$, then N_S is given as:

$$N_S = \frac{q_{avg}}{D_{avg} C_{avg}} \quad (6)$$

where q_{avg} , D_{avg} , and C_{avg} are the average of ES CPU cycles, IoT task data size, and IoT task CPU cycle requirements, respectively, in the system.

We denote the offloading strategy for IoT device I_m as $\delta_{m,k,l}$, where $\delta_{m,k,l}$ is defined as:

$$\delta_{m,k,l} = \begin{cases} 1, & \text{if } T_m \text{ is offloaded to ES } S_l \text{ via UAV } U_k \\ 0, & \text{otherwise} \end{cases} \quad (7)$$

The overall offloading strategy for the system can be represented as $\Delta = \{\delta_{m,k,l} | \forall m = 1, \dots, M, k = 1, \dots, K, \text{ and } l = 1, \dots, L\}$. When selecting an offloading strategy, the SP aims to minimize the offloading cost while satisfying the strict delay requirements of IoT tasks. For a given strategy $\delta_{m,k,l} = 1$, the offloading delay can be determined as

$$t_{m,k,l} = t_{m,k,l}^{trans} + t_l^{proc}, \\ = \left[\frac{D_{k,m}^{buffer}}{r_{m,k}} + \frac{D_m - D_{k,m}^{buffer}}{\min(r_{m,k}, r_{k,l})} + \frac{D_{k,m}^{buffer}}{r_{k,l}} \right] + \frac{D_m C_m}{q_{l,m}}, \quad (8)$$

where $t_{m,k,l}^{trans}$ is the transmission delay when offloading the task T_m from I_m to S_l via U_k and t_l^{proc} is the processing delay when executing the task T_m at S_l . Here, we are neglecting the result receiving delay from the ES to the IoTs, since the result's data size is significantly smaller compared to the input task size [9]. $D_{k,m}^{buffer}$ is the packet buffer size at UAV U_k reserved for IoT I_m (we consider that the total buffer space available at the UAV is reserved in equal proportion for all associated IoTs). $q_{l,m}$ denotes the computing resources at S_l assigned for task T_m . The task offloading is successful, if $t_{m,k,l} < \tau_m$. We further analyze the SP's profit as follows.

1) *SP Profit*: The IoT users pay price for successful offloading of their computation-intensive tasks, which we consider as the revenue for the SP. We assume, similar to [8], [9], that the price offered by an IoT user is directly proportional to the task size and inversely proportional to the delay deadline. Hence, the SP's revenue for an offloading decision $\delta_{m,k,l} = 1$, is given as:

$$\mathcal{R}_{m,k,l} = \mathcal{P}_m = v \frac{D_m}{\tau_m}, \quad (9)$$

where \mathcal{P}_m denotes the price paid by IoT I_m and v is the unit data rate price parameter (arbitrarily and theoretically assumed to be dollar/Mbps). However, at the same time, the SP hires computing resources from the ES owners for task execution and pays for it. Similar to (9), we assume that the cost paid by the SP depends both on the task size as well as the processing capacity of the hired ES [8], [9]. Hence, the cost incurred by the SP for an offloading decision $\delta_{m,k,l} = 1$ is given as:

$$\mathcal{C}_{m,k,l} = w \frac{D_m}{t_l^{proc}}, \quad (10)$$

where w [dollar/Mbps] is the price parameter [9]. The SP's profit for the offloading decision $\delta_{m,k,l} = 1$, can be defined as:

$$\mathcal{P}_{m,k,l} = \mathcal{R}_{m,k,l} - \mathcal{C}_{m,k,l}, \quad (11)$$

Here, we consider $v \gg w$. Therefore, for any successful offloading (i.e., $\delta_{m,k,l} = 1$), $\mathcal{R}_{m,k,l} > \mathcal{C}_{m,k,l}$. This implies, $\mathcal{P}_{m,k,l} > 0$, i.e., a positive SP profit is incurred for each successful task offloading. In addition to the task offloading cost, the SP has to incur a UAV operating cost which is proportional to the number of UAVs employed. Thus, given a specific network topology and a fixed offloading strategy, the overall SP profit can be expressed as:

$$\mathcal{P}_{SP} = \left[\sum_{m=1}^M \sum_{k=1}^K \sum_{l=1}^L \delta_{m,k,l} \mathcal{P}_{m,k,l} - KC^{UAV} \right] \quad (12)$$

where C^{UAV} represents the operational cost of a UAV. Eqs. (10) and (11) demonstrate how the offloading decision influences the SP profit, while (12) highlights the impact of the number of UAVs. According to (10), the SP incurs a higher cost in offloading a task (with a given requirement) to a more computationally powerful ES than a lesser one. Therefore, by strategically selecting the ES, the SP can complete task

offloading at a minimal cost, maximizing its profit. Similarly, by optimizing the number of UAVs, the SP can reduce additional operating costs, thereby enhancing its overall profit.

C. Problem Formulation

The UAV-assisted IoT task offloading in urban IoT environments has two objectives, (1) Deliver offloading services with minimum UAV resources, and (2) Maximize the SP profit while meeting the IoT's requirements. Therefore, the task-offloading problem can be modeled as:

$$P1: \max_{\Delta, K, X_U, Y_U} \mathcal{P}_{SP} \quad (13a)$$

s.t.

$$\sum_{k=1}^K \sum_{l=1}^L \delta_{m,k,l} \leq 1 \quad \forall m \in \{1, 2, \dots, M\}, \quad (13b)$$

$$\sum_{m=1}^M \sum_{l=1}^L \delta_{m,k,l} \leq N_U \quad \forall k \in \{1, 2, \dots, K\}, \quad (13c)$$

$$\sum_{m=1}^M \sum_{k=1}^K \delta_{m,k,l} \leq N_S \quad \forall l \in \{1, 2, \dots, L\}, \quad (13d)$$

$$\sum_{m=1}^M \sum_{k=1}^K \sum_{l=1}^L \delta_{m,k,l} \geq \zeta M, \quad (13e)$$

$$\Gamma_{m,k}, \Gamma_{k,l} \geq \Gamma_{th}, \quad (13f)$$

$$t_{m,k,l} \leq \tau_m \quad \forall m \in \{1, 2, \dots, M\}, \quad (13g)$$

$$\delta_{m,k,l} \in \{0, 1\} \quad (13h)$$

where $X_U = \{x_{U_k}, \forall k = 1, 2, \dots, K\}$ and $Y_U = \{y_{U_k}, \forall k = 1, 2, \dots, K\}$ are the set of X-coordinates and Y-coordinates of the UAVs, respectively. The constraint (13b) specifies that each IoT can only be paired with only one UAV, and the corresponding task can only be offloaded to a single ES. Constraints (13c), and (13d) indicate the capacity constraints for the UAVs, and ESs, respectively. Constraint (13e) outlines the minimum service demand of the system. (13f) and (13g) highlight the SINR and delay criteria for selecting a suitable IoT-UAV-ES offload pair.

IV. PROBLEM ANALYSIS AND SOLUTION DESIGN

The optimization problem $P1$ is combinatorial and NP-hard due to binary constraints (13h) and the strong coupling between variables. To solve this effectively, we decompose $P1$ into two subproblems: offloading strategy optimization ($P2$) and UAV topology optimization ($P4$). Given an initial UAV topology, $P2$ seeks the best IoT-UAV-ES associations that satisfy SINR, delay, and capacity constraints. Given the offloading strategy from $P2$, $P4$ adjusts the UAV network topology to maximize coverage while reducing UAV count. Next, we discuss these subproblems in further details.

A. Offloading Strategy Optimization

Given, a fixed UAV network topology, we can find the optimal IoT-UAV-ES associations by solving the following optimization problem.

$$P2: \max_{\Delta} \mathcal{P}_{SP} \quad (14a)$$

s.t.

$$(13b), (13c), (13d), (13f), (13g), (13h) \quad (14b)$$

Solving the above optimization problem is NP-hard [41]. Therefore, we adopt a preference-based stable matching model known as Three-sided Matching with Size and Cyclic Preference (TMSC) [42], to solve the problem. The TMSC model is used to handle scenarios having cyclic relationships among matching agents. In the context of our UAV-assisted MEC system, we observe a similar cyclic relationship among the communicating agents' preferences. The IoT devices offload their tasks to specific UAVs that provide better SINR. Therefore, IoT devices exhibit preferences only for UAVs. The UAVs forward the offloaded tasks to suitable ESs that maximize the SP's profit while satisfying the task requirements. So, the UAVs exhibit preferences over ESs only. Similarly, the ESs preferentially select IoTs that have less task computational complexity so that they can complete the task faster and accommodate more users, thus increasing the revenue. Hence, the preference lists of IoTs, UAVs, and ESs exclusively consist of UAVs, ESs, and IoT devices, respectively. This cyclic preference structure highlights the relevance of employing the TMSC model to solve our offloading strategy optimization problem $P2$ effectively.

By using TMSC, we aim to find maximum number of matching triplets (IoT-UAV-ES pairs) that maximize the system objective while satisfying the system constraints. The set of matching triplets is denoted as $\mathcal{M}_t = \{(I_m, U_k, S_l) | \delta_{m,k,l} = 1 \forall I_m \in \mathcal{I}, \forall U_k \in \mathcal{U}, \forall S_l \in \mathcal{S}\}$. Each successful task offload corresponds to a unique triplet (I_m, U_k, S_l) in \mathcal{M}_t that yields a positive profit for the SP, i.e. $\mathcal{P}_{m,k,l} > 0$. Therefore, for a given network topology (i.e., with fixed operation cost), we can maximize the SP profit by maximizing the number of matching triplets. Hence, we can reformulate the problem $P2$ as follows:

$$P3: \max_{\Delta} |\mathcal{M}_t| \quad (15a)$$

s.t.

$$\mathcal{N}(\mathcal{M}_t, U_k) \leq N_U \quad \forall k \in \{1, 2, \dots, K\}, \quad (15b)$$

$$\mathcal{N}(\mathcal{M}_t, S_l) \leq N_S \quad \forall l \in \{1, 2, \dots, L\}, \quad (15c)$$

$$\mathcal{N}(\mathcal{M}_t, I_m) \leq 1 \quad \forall m \in \{1, 2, \dots, M\}, \quad (15d)$$

$$t_{m,k,l} \leq \tau_m \quad \forall m \in \{1, 2, \dots, M\}, \quad (15e)$$

$$\Gamma_{m,k}, \Gamma_{k,l} \geq \Gamma_{th} \quad (15f)$$

The objective is to maximize the number of matched triplets in the matching set \mathcal{M}_t . $\mathcal{N}(\mathcal{M}_t, x)$ represents the number of times agent x appears in the matching set \mathcal{M}_t . Constraints (15b) and (15c) represent the limitation on the maximum number of IoTs supported by the UAV and ES, respectively. The constraint (15d) ensures that each IoT device should form only a single triplet, i.e., the IoT device I_m can only be associated with one UAV and its task can be offloaded to a single ES. The matching triplets must comply with the maximum delay and minimum SINR constraints, as indicated by condition (15e) and (15f), respectively.

Finding a stable matching set for a given instance of TMSC is an NP-hard problem [42]. Therefore, we reduce the computational complexity by imposing certain restrictions into the TMSC model and devise a Restricted-TMSC (R-TMSC) based algorithm to solve the task offloading problem. The

preference lists of all agents are derived from the master preference lists available at the MBS. The master list is a collection of agents with strict order in the form of a single or a group of lists. The master preference list of IoTs is a set of M lists, where each list corresponds to a distinct IoT device and is a collection of all UAVs, arranged in the descending order of their SINR value, $\Gamma_{m,k}$. Similarly, the master preference list of UAVs is a single list having all the ESs arranged in the ascending order of their task computing capacity, q_l . The master preference list of ESs contains all the IoTs arranged in the ascending order of their task complexity, $D_m C_m$. The preference lists of individual IoT, UAV, and ES are prepared by including all or just part of the master list agents.

The preference lists of IoTs are generated by including the UAVs from the master list that have SINR greater than the minimum SINR required for efficient data transmission (i.e., Γ_{th}). The preference list is defined as

$$PL_{I_m} = \{(u_1, u_2, \dots, u_K) | u_k = U_j, u_{k'} = U_{j'}, k < k', \forall k, k' \in [1, K], \Gamma_{m,j} \geq \Gamma_{m,j'} \geq \Gamma_{th}, \forall U_j, U_{j'} \in \mathcal{U}, j \neq j'\} \quad (16)$$

$\forall m \in \{1, 2, \dots, M\}$. The set of preference lists of all IoTs is denoted as $PL_I = \{PL_{I_m}, m = 1, 2, \dots, M\}$. Similarly, the preference lists of UAVs can be derived using Eq. (17) based on the master list that ranks all the ESs according to their processing capacity.

$$PL_{U_k} = \{(s_1, s_2, \dots, s_L) | s_l = S_v, s_{l'} = S_{v'}, l < l', q_v \leq q_{v'}, \forall l, l' \in [1, L], \forall S_v, S_{v'} \in \mathcal{S}, v \neq v' \text{ and } q_{v,k}, q_{v',k} > 0\} \quad (17)$$

$\forall k \in \{1, 2, \dots, K\}$. Let $PL_U = \{PL_{U_k}, k = 1, 2, \dots, K\}$ be the set of preference lists of all UAVs in the system. The ESs' preference lists is defined as:

$$PL_{S_l} = \{(i_1, i_2, \dots, i_M) | i_m = I_r, i_{m'} = I_{r'}, m < m', D_r C_r \leq D_{r'} C_{r'}, \forall m, m' \in [1, M], \forall I_r, I_{r'} \in \mathcal{I}, \text{ and } r \neq r'\} \quad (18)$$

$\forall l \in \{1, 2, \dots, L\}$. $PL_S = \{PL_{S_l}, l = 1, 2, \dots, L\}$ is the set of preference lists of all ESs in the system. With the knowledge of preference lists, we propose a R-TMSC motivated algorithm to find stable matching triplets that satisfy both task requirements and SP's objectives.

1) *R-TMSC based Matching Algorithm*: Algorithm 1 is the matching algorithm that solves the problem P3. Given a matching \mathcal{M}_t and any triplet $(I_m, U_k, S_l) \in \mathcal{M}_t$, we denote $\mathcal{M}_t(I_m) = U_k$, $\mathcal{M}_t(U_k) = S_l$, and $\mathcal{M}_t(S_l) = I_m$. Let

$$\mathcal{Z}_{I_m} = \{U_k | U_k \succ \mathcal{M}_t(I_m), U_k \in PL_{I_m}, \text{ and } \mathcal{N}(\mathcal{M}_t, U_k) < N_U\}, \quad (19)$$

be the set of UAVs that are preferred by IoT I_m over its current match $\mathcal{M}_t(I_m)$ and have available resources (PRBs) to provide offloading services. When $\mathcal{M}_t(I_m) = \phi$, we set $\mathcal{Z}_{I_m} = PL_{I_m}$. Similarly,

$$\mathcal{Z}_{U_k} = \{S_l | S_l \succ \mathcal{M}_t(U_k), \text{ and } S_l \in PL_{U_k}\}, \quad (20)$$

denotes the set of ESs that the UAV U_k prefers to its current match $\mathcal{M}_t(U_k)$. For $\mathcal{M}_t(U_k) = \phi$, we set $\mathcal{Z}_{U_k} = PL_{U_k}$.

$$\hat{\mathcal{Z}}_{I_m} = \{S_l | I_m \in PL_{S_l}, \mathcal{N}(\mathcal{M}_t, S_l) < N_S, \text{ and } t_{m,k,l} < \tau_m\}, \quad (21)$$

represents the set of ESs, which have the capacity to accept the task request from I_m while satisfying the delay requirement of the task T_m . Then,

$$\mathcal{Z}_{I_m}^* = \{U_k : \mathcal{Z}_{U_k} \cap \hat{\mathcal{Z}}_{I_m} \neq \phi, \text{ and } \mathcal{N}(\mathcal{M}_t, U_k) \leq N_U\}, \quad (22)$$

indicates the set of UAVs, for which there exists an ES in their preference list that can accept the task request from I_m . These sets are created (and maintained) at the BS and are updated whenever the matching set gets updated. The matching triplets of IoTs, UAVs, and ESs are derived using Algorithm 1.

Algorithm 1 takes input as the IoT, UAV, and ESs' position information (Q_I, Q_S, X_U, Y_U, H), IoTs' task requirement information (\mathcal{T}), and ESs' computation resource (\mathcal{F}) information. It returns the offloading strategy (Δ) as output. The algorithm first generates preference lists for each system agent (i.e., PL_I, PL_U, PL_S). These lists are then provided as arguments to the matching function TMSC_MATCH, which produces a stable matching set \mathcal{M}_t using an iterative approach. The function TMSC_MATCH starts with an empty matching set \mathcal{M}_t and progressively updates it during each iteration. In each iteration, the *for* loop finds better agents (UAVs and ESs) for the IoTs and updates the matching set \mathcal{M}_t with the better triplets. For any IoT I_m , $U^* \neq \phi$ indicates that a better triple exists. U^* and S^* are the set of UAVs and ESs, respectively that I_m prefers over its current match. $Head(U^*, I_m)$ and $Head(S^*, U_k)$ select the highest priority elements in the list U^* and S^* , with respect to I_m and U_k respectively. Finally, the better triple is added to the matching set \mathcal{M}_t by removing the existing one. This process repeats until we obtain a stable matching set. This stable matching set \mathcal{M}_t is an input for the OFFLOAD_STRATEGY function that produces the offload strategy Δ based on the elements of \mathcal{M}_t .

B. UAV topology Optimization

The UAV topology optimization problem can be given as:

$$P4 : \max_{K, X_U, Y_U} \mathcal{P}_{SP} \quad (23a)$$

s.t.

$$(13c), (13e), (13h) \quad (23b)$$

Note that finding an optimal solution for the problem P4 is difficult due to coupling between the variables. The number of UAVs explicitly depends upon the UAV locations, and conversely, the positioning of the UAVs is influenced by the number of UAVs. Therefore, to solve the problem, we propose a K-means-based iterative algorithm. We start with the current UAV topology and iteratively update the number of UAVs till the constraints are met. Once we find the number of UAVs, the positions of UAVs are determined using the K-means method.

K-means ensures that the UAV is positioned at the central location within the cluster, allowing it to effectively serve all users within its vicinity with minimum delay. Hence, for a cluster CL_k , the respective UAV location (x_{U_k}, y_{U_k}) can be determined by solving P5.

$$P5 : \min_{x_{U_k}, y_{U_k}} \sum_{I_m \in \mathcal{I}_{CL_k}} (x_{U_k} - x_{I_m})^2 + (y_{U_k} - y_{I_m})^2, \quad (24)$$

Algorithm 1: R-TMSC based offloading strategy

Input: $Q_I, Q_S, X_U, Y_U, H, \mathcal{T}, \mathcal{F}$

1) Prepare preference list sets PL_I, PL_U, PL_S

Function I: TMSC_MATCH (PL_I, PL_U, PL_S):

- 1) **Initialize** $\mathcal{M}_t = \phi$, and $flag = 1$;
- 2) **Find matching triplets**
 - while** $flag == 1$ **do**
 - $flag = 0$;
 - for** $m = 1$ **to** M **do**
 - $U^* = \mathcal{Z}_{I_m} \cap \mathcal{Z}_{I_m}^*$;
 - if** $U^* \neq \phi$ **then**
 - $U_k = Head(U^*)$;
 - $S^* = \mathcal{Z}_{U_k} \cap \hat{\mathcal{Z}}_{I_m}$;
 - $S_l = Head(S^*)$;
 - if** $\mathcal{N}(\mathcal{M}_t, I_m) == 1$ **then**
 - $\mathcal{M}_t = \mathcal{M}_t \setminus \{I_m, \mathcal{M}_t(I_m), \mathcal{M}_t(\mathcal{M}_t(I_m))\}$;
 - $\mathcal{M}_t = \mathcal{M}_t \cup \{I_m, U_k, S_l\}$
 - $flag = 1$;
- return** \mathcal{M}_t

Function II: OFFLOAD_STRATEGY (\mathcal{M}_t):

- 1) **Find offloading strategy**
 - for** $m = 1$ **to** M **do**
 - for** $k = 1$ **to** K **do**
 - for** $l = 1$ **to** L **do**
 - if** $\{I_m, U_k, S_l\} \in \mathcal{M}_t$ **then**
 - $\delta_{m,k,l} = 1$
 - else**
 - $\delta_{m,k,l} = 0$
- return** Δ

where \mathcal{I}_{CL_k} denotes the set of IoTs included in the cluster CL_k . The above problem is convex and the optimal solution can be obtained by equating the first-order derivative to zero [13]. So, the UAV location becomes:

$$x_{U_k} = \frac{1}{N_{CL_k}} \sum_{I_m \in \mathcal{I}_{CL_k}} x_{I_m}, \text{ and } y_{U_k} = \frac{1}{N_{CL_k}} \sum_{I_m \in \mathcal{I}_{CL_k}} y_{I_m} \quad (25)$$

where N_{CL_k} is the number of IoTs in the cluster CL_k . After finding the horizontal locations, the UAVs are deployed at predefined height H at these locations. The details of topology updation is given in the Algorithm 2. The algorithm finds a feasible UAV topology solution that ensures ζ percent IoTs are served with their offloading requirements. In order to optimize the number of UAVs, we iteratively update the number of UAVs based on the number of served IoTs. When the number of served IoTs exceeds the threshold limit, we try to optimize the number of UAVs by eliminating the one whose elimination does not affect the system performance (i.e., the served IoT percentage does not go below the threshold limit). For this, we first identify the UAV serving the least number of IoTs, and then, eliminate the same after checking the constraint. This step is repeated till the number of UAVs converges. Similarly, when the number of served IoTs is less than the threshold limit, we increase the UAV count by a minimum number that is sufficient to meet ζ percent service criteria. $max(1, \lfloor \frac{M - |S_{serve}|}{N_U} \rfloor)$ gives the additional number of required to serve the non-served users. After finding the number of UAVs, we decide their positions using K-means method.

Algorithm 2: Iterative Algorithm for UAV Topology

Input: Δ, K, ζ

Function I: UAV_Topology (Δ, K, ζ):

- 1) **Initialize** $flag = 1$;
- 2) **Update** $S_{serve} = \{I_m | \delta_{m,k,l} = 1, \forall k, l\}$;
- 3) **Update number of UAVs and their positions**
 - while** $flag == 1$ **do**
 - $flag = 0$;
 - if** $|S_{serve}| > \zeta M$ **then**
 - for** $k = 1$ **to** K **do**
 - $S_{serve}^k = \{I_m | I_m \in S_{serve}, \delta_{m,k,l} = 1, \forall m, l\}$
 - $\hat{k} = \arg \min(|S_{serve}^k|)$;
 - if** $(|S_{serve}| - |S_{serve}^{\hat{k}}|) > \zeta M$ **then**
 - $K = K - 1$;
 - $flag = 1$;
 - $S_{serve} = S_{serve} \setminus S_{serve}^{\hat{k}}$;
 - else**
 - $K = K$;
 - else**
 - $K = K + max(1, \lfloor \frac{M - |S_{serve}|}{N_U} \rfloor)$
 - for** $k = 1$ **to** K **do**
 - Compute x_{U_k} and y_{U_k} using (25);
 - return** K, X_U, Y_U

Algorithm 3 shows the joint optimization of UAV topology and offloading strategy for efficient task offloading. We start with an initial UAV topology. The initial topology should be selected such that the algorithm converges with minimum iterations. So, we assume that each UAV serves at its maximum capacity, i.e, N_U , and estimate the initial number of UAVs as

$$K_{initial} = \left\lfloor \frac{M}{N_U} \right\rfloor \quad (26)$$

where $\lfloor \cdot \rfloor$ is the floor operator. With the initial topology, we iteratively update the offloading strategy and the topology, till the profit converges.

Algorithm 3: Joint Optimization of Topology and Offloading Strategy for Profit Maximization

Input: $Q_I, Q_S, N_U, H, f, c, \mu_{LoS}, \mu_{NLoS}, \zeta, a, b$

- 1: Determine initial no. of UAVs ($K_{initial}$) using (26);
- 2: Find initial UAV positions using (25);
- 3: **Initialize** $K = K_{initial}, iter = 0, flag = 1$;
- 4: **Set** $\mathcal{P}_{SP}(iter) = 0$;
- 5: **Update** UAV topology and offloading strategy iteratively;
 - while** $flag == 1$ **do**
 - $flag = 0$;
 - $iter = iter + 1$;
 - Update Δ using Algorithm 1;
 - Find $\mathcal{P}_{SP}(iter)$ using (12);
 - if** $\mathcal{P}_{SP}(iter) - \mathcal{P}_{SP}(iter - 1) < \epsilon$ **then**
 - $\Delta^* = \Delta, K^* = K, X_U^* = X_U, Y_U^* = Y_U$
 - else**
 - Update K, X_U and Y_U using Algorithm 2;
 - $flag = 1$;

Output: K^*, X_U^*, Y_U^* , and Δ^*

Algorithm 1 involves sequential matching of the preference list elements. Therefore, in the worst case where the elements

are matched one by one, the algorithm has a computational complexity of $n_1 \times \mathcal{O}(MKL)$, where n_1 is the number of iterations that the algorithm 1 takes to converge. Similarly, algorithm 2 has a complexity order of $n_2 \times \mathcal{O}(K)$ with n_2 being the number of iterations required for convergence of algorithm 2. So, if algorithm 3 takes n iteration to converge, then the overall computational complexity of the proposed algorithm can be expressed as $n \times [\mathcal{O}(n_1MKL) + \mathcal{O}(n_2K)]$.

V. PERFORMANCE ANALYSIS

A simulation-based comprehensive performance analysis of our proposed task offloading scheme is carried out using MATLAB R2022b. We evaluate the effectiveness of our proposed strategy in comparison to two benchmarks: Fixed [39] and Random offloading [21]. In fixed offloading, the IoT-UAV-ES associations are fixed, wherein the IoT device first offloads its task to the corresponding cluster UAV, which then forwards it to the nearest ES for execution. On the other hand, the random offloading allows task offloading without any predefined association plan. Together, these benchmarks provide a balanced perspective on performance across both controlled and dynamic urban MEC settings. We keep resource allocation consistent across all schemes for a fair comparison, and analyze the impact of different IoT-UAV-ES association strategies on system performance.

A. Simulation Framework

We create a simulation environment for an area of 1km^2 . The BS is placed at the center of the region and the IoT devices are distributed uniformly randomly across the region [13]. The ESs are located at predetermined fixed positions to facilitate the MEC services for IoT devices [21]. To assist MEC service provision, the UAVs are deployed at a predetermined altitude [17]. The location of UAVs are determined using the K-means algorithm [13]. The parameter settings for the simulation are summarized in Table III [8], [9], [17], [20], [21], [39]. The task computing capacity of the ESs (N_S) are selected within the range [10, 50] tasks/s, and the price parameters are set as, $v = 0.1$ and $w = 0.01$ dollars/Mbps.

Parameters	Values
UAV operating height (H)	100 m
Power gain at reference distance (β_o)	10^{-3}
Threshold SINR (Γ_{th})	3dB
Noise power (N_0)	-170 dBm
IoT transmit power (P_m)	[100, 500] mW
UAV transmit power (P_k)	1 W
Data size of task (D_m)	[2, 5] MB
CPU cycle requirement of task (C_m)	[100,200] cycles/bit
Maximum task completion delay (τ_m)	[2, 5] s
Task arrival rate	30 tasks/min
Computing resource of ES (q_l)	[8, 10] GHz
Bandwidths of PRB (B_1)	180 KHz
Number of PRBs (Z)	100
UAV to ES transmission bandwidth (B_2)	5 MHz
Maximum IoT user capacity of UAV (N_U)	[10, 20]

TABLE III: Simulation parameters for performance evaluation

With these simulation settings, we first evaluate the convergence of the proposed task offloading algorithm with $N_U = 20$ and $N_S = 40$. Then, we perform Monte-Carlo simulation with

a 95 % confidence interval for the configurations listed in table IV. We evaluate the system performance in terms of percentage of served IoTs, SP profit, and average user satisfaction. Since the proposed offloading aims to meet strict delay requirements of IoT tasks, we consider offloading latency for measuring user satisfaction [9]. For offloading strategy $\delta_{m,k,l} = 1$, we model the user satisfaction as a logarithmic function [43], given as:

$$\mathcal{V}_{m,k,l} = \begin{cases} \log\left(1 + \frac{\tau_m}{t_{m,k,l}}\right), & \text{if } 0 < t_{m,k,l} < \tau_m \\ 0, & \text{otherwise} \end{cases} \quad (27)$$

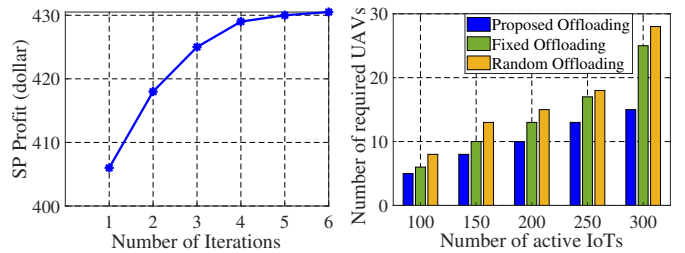
Configurations	$ Z $	$ S $
Set 1	100, 150, . . . , 300	8
Set 2	200	2, 4, . . . , 10

TABLE IV: Experiment configurations. Set 1 and 2 has increasing number of IoTs and ESs, respectively.

B. Performance Analysis

1) Algorithm convergence and UAV requirement analysis:

Fig. 2(a) shows the convergence pattern of the proposed iterative algorithm with $M = 200$, $L = 8$, $N_U = 20$ and $N_S = 40$. The SP profit increases with the number of iterations, and stabilizes just after four iterations. Each iteration executes in 18 ms and the algorithm converges within 60 ms on a Lenovo ThinkPad E14 with an Intel i5 processor. Overall, deploying the proposed solution in urban environments incurs a small ($< 60\text{ms}$) execution-time overhead.



(a) Convergence performance of proposed algorithm with $M = 200$, $L = 8$, $N_U = 20$, $N_S = 40$. (b) Number of required UAVs with increasing number of active IoTs for $\zeta = 90\%$

Fig. 2: Algorithm convergence and UAV requirement analysis

The minimum number of required UAVs with the proposed and the benchmark schemes is shown in Fig. 2(b). We set the minimum served IoT percentage threshold as $\zeta = 90\%$ and evaluate the number of UAVs required under configuration set 1, with parameters $N_U = 20$ and $N_S = 40$. The number of required UAVs is greater for a higher number of IoTs. However, our proposed scheme effectively serves the required number of IoTs with fewer UAVs as compared to the benchmark schemes, thereby improving the SP profit.

2) *Effect of increasing number of active IoTs:* The system performance for an increase in the number of active IoTs using configuration set 1 is shown in Fig. 3. Fig. 3(a) shows the percentage of served IoTs, that decreases with an increase in the number of active IoTs. This is due to an increased competition between the devices to obtain their preferred triplets with a higher number of active IoTs in the system. It may leave some of the devices out of pairing due to the capacity constraints of UAVs and ESs, leading to a decrease in the served percentage. Fig. 3(b) shows the effect on SP

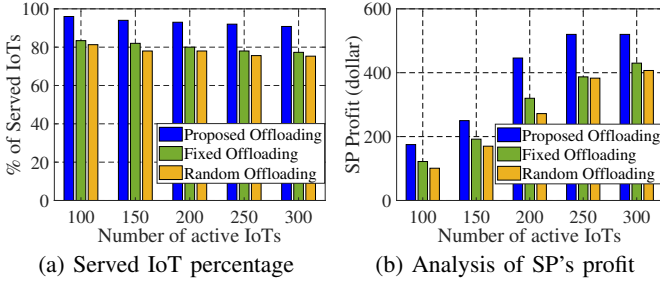


Fig. 3: Performance with increase in number of active IoTs

profit. The SP profit increases as the number of active IoTs increases. However, the rate of growth gradually slows down. This is because as the number of active IoTs increases, there is a saturation point after a certain threshold number of IoTs (currently at 250) where the system reaches its maximum capacity. Beyond this point, further increase in the number of active IoTs has minimal impact on the SP profit.

We note that our proposed offloading strategy achieves an average served percentage of 93.4 %, much higher than 80.1 % for Fixed and 77.6 % for Random offloading schemes. Also, the SP profit with the proposed offloading is 21% and 28% higher than the fixed and random strategies, respectively. This performance improvement with our scheme is attributed to the preference-based task offloading and the provision for less preferred pairs when more preferred choices are unavailable.

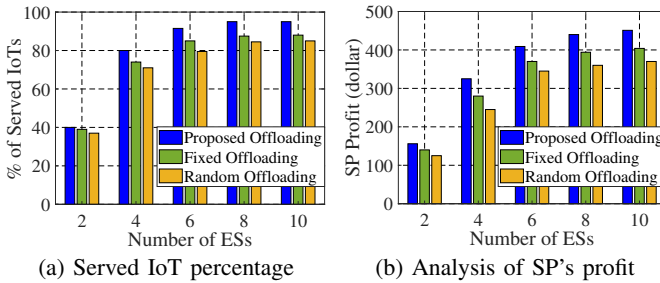


Fig. 4: Performance with increase in number of ESs

3) *Effect of increasing number of ESs*: Fig. 4 shows system performance with an increase in the number of ESs, based on the configuration set 2. We fix number of UAVs as $K = K_{initial} = 10$, evaluated using (26) with $M = 200$, and $N_U = 20$. Fig. 4(a) shows the percentage of served IoTs that initially increases due to the formation of more matching triplets. However, due to fixed UAV capacity, the system becomes saturated after a certain number of ESs (8 in this case). Therefore, adding more ESs beyond this point does not lead to any significant improvement in system performance, resulting in a constant served IoT percentage. Fig. 4(b) provides insights into the SP's profit. The graph shows the SP profit increases with the number of ESs. This is because as the number of ESs increases, the chance of UAVs being matched with their preferred ESs also increases, which reduces the task execution cost and thereby leads to an improvement in the SP's profit. However, the rate of growth in the performance metric becomes slower beyond 8 ESs, indicating that the system approaches a saturation point. Overall, the performance improvement with increasing number of ESs is constrained by the capacity of UAVs. This can be considered to determine an

appropriate number of ESs (in this case it is 8) to achieve a balance between the benefits of increasing the number of ESs and the constraints of the UAV's capacity.

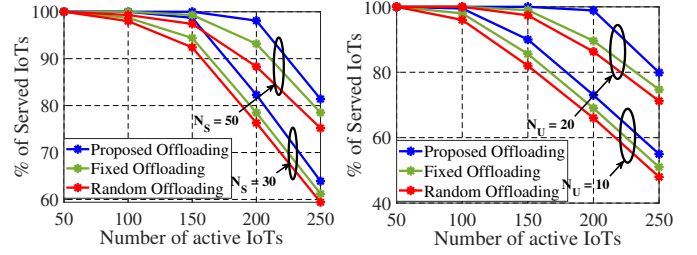


Fig. 5: Server and UAV capacity impact on performance.

4) *Effect of the server and UAV capacity*: Fig. 5 shows the system performance with different ES's computing and UAV's serving capacities for the configuration set 1. In Fig. 5(a), the percentage of served IoTs is shown for two different task computing capacities of ES: $N_S = 30$, and $N_S = 50$, while maintaining the IoT user capacity of UAVs at $N_U = 15$. Similarly, Fig. 5(b) shows the performance for two different UAVS's serving capacity values: $N_U = 10$, and $N_U = 20$, while keeping $N_S = 40$. The served IoT percentage increases as we increase the ES and UAV capacities that results in more matching triplets being formed, allowing more IoTs to successfully offload their tasks. Hence, for a given UAV-assisted MEC system, we can employ higher-capacity UAVs and ESs to improve the overall system performance.

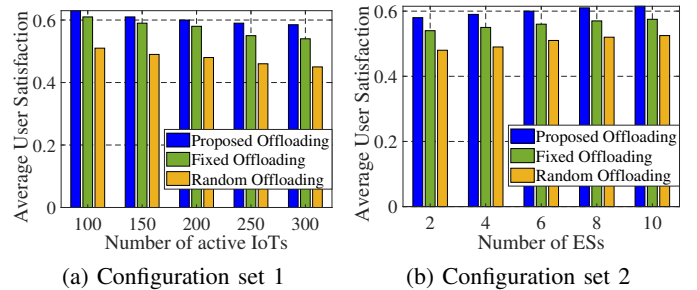


Fig. 6: User satisfaction under different configuration setup.

5) *User satisfaction Performance*: Fig. 6 shows the average user satisfaction performance for the configuration sets 1 and 2. We note from Fig. 6(a) that as the number of IoTs increases, the average user satisfaction decreases due to an increased competition among devices to obtain their preferred pairs (UAVs and ESs). However, the reduction rate becomes less pronounced beyond 250 IoTs, which can be attributed to the saturation state of the system due to the capacity constraints at the UAV and the ES level. Figs. 6(b) shows the variation of average user satisfaction with the increasing number of ESs. As the number of ESs increases, the average user satisfaction increases, which is due to the increased system capacity that allows the UAVs to offload the tasks to their preferred ESs. Furthermore, the increase in the number of ESs decreases the effective distance between the UAV and its preferred ES. This reduction in distance subsequently decreases the task transmission delay, which ultimately improves the average

user satisfaction. We notice from Figs. 6(a) and 6(b) that our proposed offloading approach delivers better user satisfaction than the benchmark schemes.

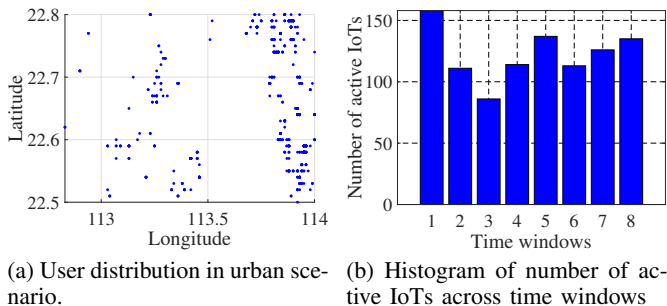


Fig. 7: Simulation scenario based on real-world data

6) *System performance based on real-world data:* In the above simulation, we have assumed a uniform distribution of IoT devices across the desired area. However, real-world user distribution may not always follow this uniform pattern. Therefore, to ensure the robustness and applicability of our algorithm, we aim to validate our system performance using real-world data. For this, we consider the China Mobile User Geographics data set that provides information about mobile user activities, including timestamps and geographical coordinates [44]. We select a densely populated region bounded by latitude 22.5 to 23.3, and longitude 112.5 to 114.8. Fig. 7(a) shows the mobile user distribution in this region between 10 AM to 12 PM. Based on this user distribution, we deploy 8 ESs at strategic locations to support task offloading services. The locations of these ESs are (22.775, 113.8), (22.725, 113.85), (22.675, 113.85), (22.6, 113.85), (22.55, 113.85), (22.55, 113.4), (22.6, 113.2), and (22.7, 113.25). We divide the entire duration into 15-minute time windows and analyze the system performance across each window. The histogram in Fig. 7(b) illustrates the variation in number of active IoTs over each window.

Fig. (8) shows the evaluation results of performance metrics for different schemes with $N_U = 20$ and $N_S = 40$. Fig. 8(a) compares the percentage of served IoTs of the proposed offloading with the benchmark schemes across different time windows, while Fig. 8(b) and 8(c) compare the SP profit and average user satisfaction over these intervals, respectively. The proposed strategy outperforms both the fixed and the random offloading in terms of the percentage of served IoTs, SP profit, and average user satisfaction. It achieves an average of 10% and 28% higher served percentage than the fixed and random strategy, respectively. Similarly, the SP profit with the proposed strategy becomes 1.2 times and 1.5 times higher than the fixed and random strategy, respectively.

Overall, our proposed offloading solution for a UAV-assisted MEC system provides a higher percentage of served IoTs than the benchmark schemes. Since it serves a larger number of IoT users, it is suitable for the urban IoT networks. Furthermore, it improves the SP revenue by an average of 19% along with an improvement in user satisfaction (by 12%), thereby satisfying the needs of both users as well as the SP. Remarkably, the number of required UAVs to achieve this performance improvement is nearly 25% lesser in the proposed scheme

compared to the benchmark scheme.

VI. CONCLUSION

In this article, we have presented the UAV-assisted MEC architecture that supports IoT task offloading in urban environments. Our proposed architecture efficiently fulfills the latency and computational demands of IoT devices by deploying UAVs as relay nodes and utilizing ground ESs, combining both to achieve a robust solution that maximizes user satisfaction and SP profit. We use a three-sided matching optimization and an efficient UAV network deployment strategy to find a stable match between IoTs, UAVs, and ESs while utilizing the the minimum number of UAVs. Our proposed UAV-assisted MEC based IoT task offloading scheme is effective in urban environments and offers an average improvement of 19%, 12%, and 25% in the percentage of served IoTs, average user satisfaction, and SP profit, respectively, as compared to its benchmarks.

REFERENCES

- [1] T. Taleb, N. Sehad, Z. Nadir, and J. Song, "VR-based immersive service management in B5G mobile systems: A UAV command and control use case," *IEEE Internet of Things J.*, vol. 10, no. 6, pp. 5349–5363, 2023.
- [2] W. U. Rahman, Y.-S. Choi, and K. Chung, "Performance evaluation of video streaming application over coop in iot," *IEEE Access*, vol. 7, pp. 39852–39861, 2019.
- [3] Y. He, D. Zhai, R. Zhang, J. Du, G. S. Aujla, and H. Cao, "A mobile edge computing framework for task offloading and resource allocation in UAV-assisted VANETs," in *Proc. IEEE INFOCOM Wksp.*, 2021.
- [4] Y. Mao, C. You, J. Zhang, K. Huang, and K. B. Letaief, "A survey on mobile edge computing: The communication perspective," *IEEE Commun. surveys & tutorials*, vol. 19, no. 4, pp. 2322–2358, 2017.
- [5] J. Yang, Q. Yuan, S. Chen, H. He, X. Jiang, and X. Tan, "Cooperative task offloading for mobile edge computing based on multi-agent deep reinforcement learning," *IEEE Trans. Netw. Serv. Manag.*, vol. 20, no. 3, pp. 3205–3219, 2023.
- [6] A. Tian, B. Feng, H. Zhou, Y. Huang, K. Sood, S. Yu, and H. Zhang, "Efficient federated DRL-based cooperative caching for mobile edge networks," *IEEE Trans. Netw. Serv. Manag.*, vol. 20, no. 1, pp. 246–260, 2023.
- [7] H. Chang, Y. Chen, B. Zhang, and D. Doermann, "Multi-UAV mobile edge computing and path planning platform based on reinforcement learning," *IEEE Trans. Emerging Topics in Computational Intelligence*, vol. 6, no. 3, pp. 489–498, 2022.
- [8] A. Pratap, "Cyclic stable matching inspired resource provisioning for iot-enabled 5G networks," *IEEE Trans. Veh. Tech.*, vol. 71, no. 11, pp. 12195–12205, 2022.
- [9] Y. Gu, Z. Chang, M. Pan, L. Song, and Z. Han, "Joint radio and computational resource allocation in iot fog computing," *IEEE Trans. Veh. Tech.*, vol. 67, no. 8, pp. 7475–7484, 2018.
- [10] Y. Dai, D. Xu, S. Maharjan, and Y. Zhang, "Joint computation offloading and user association in multi-task mobile edge computing," *IEEE Trans. Veh. Tech.*, vol. 67, no. 12, pp. 12313–12325, 2018.
- [11] I. Rafiq, A. Mahmood, S. Razzaq, S. H. M. Jafri, and I. Aziz, "IoT applications and challenges in smart cities and services," *The Journal of Engineering*, vol. 2023, no. 4, p. e12262, 2023.
- [12] Y. Huo, X. Dong, W. Xu, and M. Yuen, "Cellular and WiFi co-design for 5G user equipment," in *Proc. IEEE 5GWF*, pp. 256–261, 2018.
- [13] S. Barick and C. Singhal, "Multi-uav assisted IoT NOMA uplink communication system for disaster scenario," *IEEE Access*, vol. 10, pp. 34058–34068, 2022.
- [14] G. Reus-Muns, M. Diddi, C. Singhal, H. Singh, and K. R. Chowdhury, "Flying among stars: Jamming-resilient channel selection for UAVs through aerial constellations," *IEEE Transactions on Mobile Computing*, vol. 22, no. 3, pp. 1246–1262, 2023.
- [15] A. Bist and C. Singhal, "Efficient immersive surveillance of inaccessible regions using uav network," in *Proc. IEEE INFOCOM*, pp. 1–6, 2021.
- [16] N. Kumar, M. Ghosh, and C. Singhal, "UAV network for surveillance of inaccessible regions with zero blind spots," in *Proc. IEEE INFOCOM*, pp. 1213–1218, 2020.

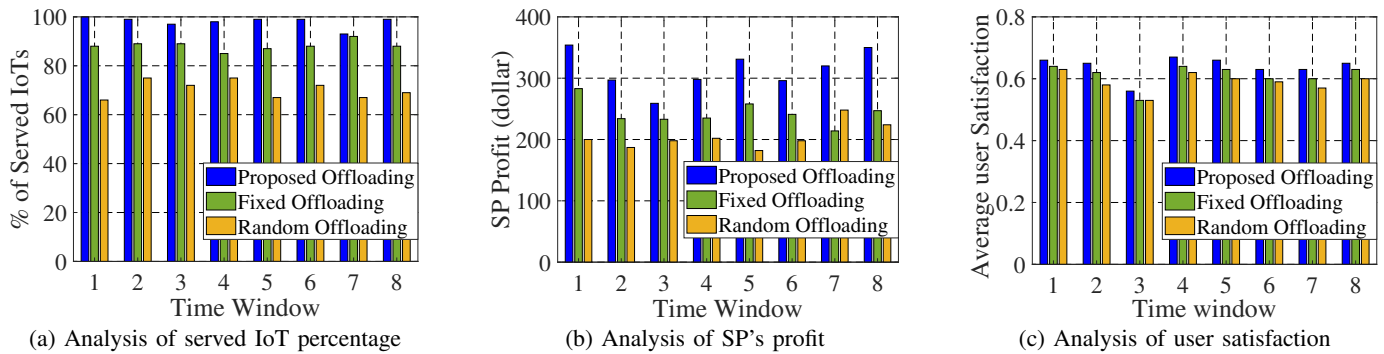


Fig. 8: System Performance with Real-world Data

- [17] C. Singhal and S. Barick, "ECMS: Energy-efficient collaborative multi-UAV surveillance system for inaccessible regions," *IEEE Access*, vol. 10, pp. 95876–95891, 2022.
- [18] C. Singhal and B. N. Chandana, "Aerial-SON: Uav-based self-organizing network for video streaming in dense urban scenario," in *Proc. COM-SNETS*, pp. 7–12, 2021.
- [19] C. Singhal and K. Rahul, "LB-UAVnet: Load balancing algorithm for uav based network using sdn," in *Proc. IEEE WPMC*, pp. 1–5, 2019.
- [20] N. N. Ei, S. W. Kang, M. Alsenwi, Y. K. Tun, and C. S. Hong, "Multi-UAV-assisted MEC system: Joint association and resource management framework," in *Proc. IEEE ICOIN*, pp. 213–218, 2021.
- [21] Z. Yu, Y. Gong, S. Gong, and Y. Guo, "Joint task offloading and resource allocation in UAV-enabled mobile edge computing," *IEEE Internet Things J.*, vol. 7, no. 4, pp. 3147–3159, 2020.
- [22] M. Dai, Z. Su, Q. Xu, and N. Zhang, "Vehicle assisted computing offloading for unmanned aerial vehicles in smart city," *IEEE Trans. Intell. Transp. Syst.*, vol. 22, no. 3, pp. 1932–1944, 2021.
- [23] M. Liwang, Z. Gao, and X. Wang, "Let's trade in the future! a futures-enabled fast resource trading mechanism in edge computing-assisted UAV networks," *IEEE J. Sel. Areas Commun.*, vol. 39, no. 11, pp. 3252–3270, 2021.
- [24] N. N. Ei, M. Alsenwi, Y. K. Tun, Z. Han, and C. S. Hong, "Energy-efficient resource allocation in multi-UAV-assisted two-stage edge computing for beyond 5G networks," *IEEE Trans. Intell. Transp. Syst.*, vol. 23, no. 9, pp. 16421–16432, 2022.
- [25] D. Kim, H. Lee, H. Song, N. Choi, and Y. Yi, "Economics of fog computing: Interplay among infrastructure and service providers, users, and edge resource owners," *IEEE Trans. Mob. Comput.*, vol. 19, no. 11, pp. 2609–2622, 2020.
- [26] L. Gao, G. Iosifidis, J. Huang, and L. Tassiulas, "Economics of mobile data offloading," in *Proc. IEEE INFOCOM*, pp. 3303–3308, 2013.
- [27] P. Trakas, F. Adelantado, and C. Verikoukis, "Network and financial aspects of traffic offloading with small cell as a service," *IEEE Trans. Wirel. Commun.*, vol. 17, no. 11, pp. 7744–7758, 2018.
- [28] J. Xu, L. Chen, and P. Zhou, "Joint service caching and task offloading for mobile edge computing in dense networks," in *Proc. IEEE INFOCOM*, pp. 207–215, 2018.
- [29] Q. Hu, Y. Cai, G. Yu, Z. Qin, M. Zhao, and G. Y. Li, "Joint offloading and trajectory design for UAV-enabled mobile edge computing systems," *IEEE Internet Things J.*, vol. 6, no. 2, pp. 1879–1892, 2019.
- [30] H. Wang, X. Wang, X. Lan, T. Su, and L. Wan, "BSBL-based auxiliary vehicle position analysis in smart city using distributed MEC and UAV-deployed IoT," *IEEE Internet Things J.*, vol. 10, pp. 975–986, 2023.
- [31] L. Zhang and N. Ansari, "Latency-aware IoT service provisioning in UAV-aided mobile-edge computing networks," *IEEE Internet Things J.*, vol. 7, no. 10, pp. 10573–10580, 2020.
- [32] C. Singhal and K. Rahul, "Efficient QoS provisioning using sdn for end-to-end data delivery in UAV assisted network," in *Proc. IEEE ANTS*, pp. 1–6, 2019.
- [33] S. Jeong, O. Simeone, and J. Kang, "Mobile edge computing via a UAV-mounted cloudlet: Optimization of bit allocation and path planning," *IEEE Trans. Veh. Tech.*, vol. 67, no. 3, pp. 2049–2063, 2018.
- [34] F. Zhou, Y. Wu, R. Q. Hu, and Y. Qian, "Computation rate maximization in UAV-enabled wireless-powered mobile-edge computing systems," *IEEE J. Sel. Areas Commun.*, vol. 36, no. 9, pp. 1927–1941, 2018.
- [35] T. Bose, A. Suresh, O. J. Pandey, L. R. Cenkeramaddi, and R. M. Hegde, "Improving quality-of-service in cluster-based UAV-assisted edge networks," *IEEE Trans. Netw. Serv. Manag.*, vol. 19, no. 2, 2022.
- [36] A. M. Seid, G. O. Boateng, B. Mareri, G. Sun, and W. Jiang, "Multi-agent DRL for task offloading and resource allocation in multi-UAV enabled IoT edge network," *IEEE Trans. Netw. Serv. Manag.*, vol. 18, no. 4, pp. 4531–4547, 2021.
- [37] Y. Xu, T. Zhang, J. Loo, D. Yang, and L. Xiao, "Completion time minimization for UAV-assisted mobile-edge computing systems," *IEEE Trans. Veh. Tech.*, vol. 70, no. 11, pp. 12253–12259, 2021.
- [38] Y. Wang, W. Chen, T. H. Luan, Z. Su, Q. Xu, R. Li, and N. Chen, "Task offloading for post-disaster rescue in unmanned aerial vehicles networks," *IEEE/ACM Trans. Netw.*, vol. 30, no. 4, pp. 1525–1539, 2022.
- [39] N. Zhao, Z. Ye, Y. Pei, Y.-C. Liang, and D. Niyato, "Multi-agent deep reinforcement learning for task offloading in UAV-assisted mobile edge computing," *IEEE Trans. Wirel. Commun.*, vol. 21, no. 9, 2022.
- [40] A. Pratap and S. K. Das, "Stable matching based resource allocation for service provider's revenue maximization in 5G networks," *IEEE Trans. Mob. Comput.*, vol. 21, no. 11, pp. 4094–4110, 2022.
- [41] A. Omran, L. Sboui, M. Kadoch, Z. Chang, J. Lu, and R. Liu, "3d deployment of multiple uavs for emergent on-demand offloading," in *Proc. IWCMC*, pp. 692–696, 2020.
- [42] L. Cui and W. Jia, "Cyclic stable matching for three-sided networking services," *Computer Networks*, vol. 57, no. 1, pp. 351–363, 2013.
- [43] M. Dai, Z. Su, J. Li, and J. Zhou, "An energy-efficient edge offloading scheme for UAV-assisted internet of things," in *Proc. IEEE ICDCS*, pp. 1293–1297, 2020.
- [44] ChinaPage, "China mobile user demographics," 2018. [Online]. Available: <https://www.kaggle.com/chinapage/china-mobile-user-demographics>.



Institute of Technology, MAHE, India. His research interests include next-generation wireless network, UAV-assisted communication, network resource management, and multi-access edge computing.



and reviewer for several top-tier ACM and IEEE conferences and journals.

Subhrajit Barick received his B.Tech. degree in Electronics and Telecommunications Engineering from Biju Patnaik University of Technology (BPUT), Odisha, India in 2013, the M.Tech. degree in Communication System Engineering from Indian Institute of Information Technology, Design and Manufacturing (IIITDM), India, in 2016. He has submitted his Ph.D. thesis in the department of Electronics and Electrical Communication Engineering, at IIT Kharagpur, India. Currently he is working as an Assistant Professor in the Manipal

Chetna Singhal [M'15, SM'21] is a Researcher at INRIA, France. She worked as an Assistant Professor at Indian Institute of Technology (IIT) Kharagpur from 2015 till 2024. She was an ERCIM Fellow at RISE, Sweden in 2022 and a visiting researcher at Northeastern University, Boston in 2018 and Politecnico di Torino, Italy in 2015 and 2016. She received her M.Tech. and Ph.D. from IIT Delhi in 2010 and 2015, respectively. Her research interests include UAV networks, machine learning orchestration, and IoT systems. She regularly serves as a TPC member